Interaction between a Slowly Moving Planetary–Scale Dipole Envelope Rossby Soliton and a Wavenumber–Two Topography in a Forced Higher Order Nonlinear Schrödinger Equation①

Luo Dehai (罗德海)

Department of Atmospheric and Oceanic Sciences, Ocean University of Qingdao, Key Laboratory of Marine Science and Numerical Modeling, State Oceanic Administration, Qingdao 266003

Li Jianping (李建平)

LASG, Institute of Atmospheric Physics, Chinese Academy of Sciences, Beijing 100029

(Received February 13, 2000; revised June 20, 2000)

ABSTRACT

A parametrically excited higher–order nonlinear Schrödinger (NLS) equation is derived to describe the interaction of a ,slowly moving planetary–scale envelope Rossby soliton for zonal wavenumber–two with a wavenumber–two topography under the LG–type dipole near–resonant condition. The numerical solution of this equation is made. It is found that in a weak background westerly wind satisfying the LG–type dipole near–resonance condition, when an incipient envelope Rossby soliton is located in the topographic trough and propagates slowly, it can be amplified through the near–resonant forcing of wavenumber–two topography and can exhibit an oscillation. However, this soliton can break up after a long time and excite a train of small amplitude waves that propagate westward. In addition, it is observed that in the soliton–topography interaction the topographically near–resonantly forced planetary–scale soliton has a slowly westward propagation, but a slowly eastward propagation after a certain time. The instantaneous total streamfunction fields of the topographically forced planetary–scale soliton are found to bear remarkable resemblance to the initiation, maintenance and decay of observed omega–type blocking high and dipole blocking. The soliton perturbation theory is used to examine the role of a wavenumber–two topography in near–resonantly forcing omega–type blocking high and dipole blocking. It can be shown that in the amplifying process of forced planetary–scale soliton, due to the inclusion of the higher order terms its group velocity gradually tends to be equal to its phase velocity so that the block envelope and carrier wave can be phase–locked at a certain time. This shows that the initiation of blocking is a transfer of amplified envelope soliton system from dispersion to nondispersion. However, there exists a reverse process during the decay of blocking. It appears that in the higher latitude regions, the planetary–scale envelope soliton–topography interaction could be regarded as a possible mechanism of the establishment of blocking.

Key words: Planetary–scale envelope Rossby soliton, Soliton–topography interaction, Blocking high

1. Introduction

Low–frequency blocking flows are very important phenomena in the atmospheric fluid (Rex,1950a,b; Shutts, 1983; McWilliams, 1980). A very interesting problem is to investigate why such structures usually occur in the North Atlantic Ocean (or Europe) and North Pacific (Charney and DeVore, 1979; Tung and Lindzen, 1979). Such studies will be very important in leading to

①This study was supported jointly by the Foundation for University Key Teacher by the Ministry of Education, the National Natural Science Foundation of China (49775266, 49905007) and the Innovation Project of IAP / CAS (8–1301).

increased understanding of atmospheric coherent structures such as blockings (McWilliams, 1980). However, presently, there is no completely satisfactory analytical theory of blocking–topography interaction. In particular, the previous studies are mainly focused on the interaction of blocking with isolated topography (Warn and Branset, 1983; Swaters, 1986). To some extent, these models are not successful in describing the location and flow pattern of observed blocking highs at high latitudes, especially in explaining why such structures can prevail in the weak background westerly wind (McWilliams, 1980; Shutts, 1983; Legras and Ghil, 1985). In a highly resolved truncated spectral model with a wavenumber–two topography, Legras and Ghil (1985) found that in a moderate range of weak background westerly wind that is near the dipole near–resonance, the blocking high can occur in the topographic trough. Thus, it would be interesting to investigate the near–resonant interaction of blocking with wavenumber–two topography in an analytical model.

Although the previous models have achieved some successes in modeling some aspects of observed blocking high and dipole blocks, there remain, however, serious questions about why most blockings occur in the two oceans where the weak basic westerly wind prevails, in particular in the high latitude region (McWilliams, 1980; Treidl et al., 1981). This means that it is necessary to establish a new analytical model of the blocking–topography interaction. Benney (1979), Yamagata (1980) and Boyd (1983) investigated envelope Rossby solitons in mid–high latitudes and at the equator. Afterwards, the dynamics of envelope Rossby soliton applicable to atmospheric blockings was studied widely by Luo (1991,1997a,1999,2000a,b). The present paper is a report on the interaction between slowly moving planetary–scale envelope Rossby soliton and wavenumber–two topography. We begin with a simplest barotropic model in order to gain insight into the most essential aspects of the blocking–topography interaction. Further studies using more realistic baroclinc models will be reported elsewhere.

This paper is organized as follows: In Section 2, in an inviscid, barotropic and quasi–geostrophic model with topography a parametrically excited higher–order nonlinear Schrödinger (HNLS) equation is obtained to describe the near–resonant interaction between planetary–scale envelope Rossby soliton and a wavenumber–two topography. In Section 3, the numerical solution of this equation is presented. In Section 4, the soliton perturbation theory used widely by many investigators (Abdullaev, 1989; Kivshar and Malomed, 1989; Hasegawa and Kodama, 1995) is used to explore why the wavenumber–two topography can reinforce and maintain blocking highs in a weak background westerly wind. The conclusion and discussions are summarized in Section 5.

2. The derivation of the parametrically excited HNLS equation

The nondimensional, nondissipative, barotropic and quasi–geostrophic potential vorticity equation with bottom topography on a beta–plane channel can be written as (Charney and Devore, 1979; Luo, 1997b, 1999)

$$\frac{\partial}{\partial t}(\nabla^2\psi - F\psi) + J(\psi, \nabla^2\psi + h) + \beta\frac{\partial\psi}{\partial x} = 0, \tag{1}$$

where the parameters and notation can be found in Luo (1999).

The flow is contained within a beta–channel on whose boundaries

$$\frac{\partial\psi}{\partial x} = 0, \quad y = 0, \quad L_y, \tag{2}$$

while the zonally averaged part of the streamfunction, $\overline{\psi}(y, t)$, must satisfy

$$\frac{\partial^2}{\partial t}\frac{\overline{\psi}}{\partial y}=0,\quad y=0,\quad L_y, \tag{3}$$

where L_y is the width of the beta–channel.

In the Northern Hemisphere (NH), the heights of nondimensional topography between 30°N and 60°N were found to correspond in turn to 0.468, 0.519, 0.343 and 0.327 for zonal wavenumbers 1–4 (Peixoto et al., 1964). Because the wavenumber–two topography is dominant and blocking flows usually exhibit a wavenumber–two structure (Charney and Devore, 1979), the large–scale topography in the Northern Hemisphere can be approximately considered as a wavenumber–two topography. On the other hand, because the topographically induced disturbance has the same order as the free linear Rossby wave (Tung and Lindzen, 1979; Luo, 1997b, 1999), the topographic assumption $h=\varepsilon h'$ should be acceptable for our study here, where $0<\gamma_0<\varepsilon<<1.0$ has been assumed with the Rossby number $\gamma_0=U/(f_0 L)\approx 0.1$ (Luo, 1997b). Consequently, we can introduce a topographic amplitude parameter ε, so that

$$\psi=-\bar{u}y+\varepsilon\psi',\quad h=\varepsilon h', \tag{4}$$

where $\bar{u}$ is the uniform basic westerly wind.

The substitution of (4) into Eq. (1) yields

$$\left(\frac{\partial}{\partial t}+\bar{u}\frac{\partial}{\partial x}\right)(\nabla^2\psi'-F\psi')+\varepsilon J(\psi',\nabla^2\psi'+h')+(\beta+F\bar{u})\frac{\partial\psi'}{\partial x}+\bar{u}\frac{\partial h'}{\partial x}=0. \tag{5}$$

If we can introduce the slowly varying coordinates (Yamagata, 1980; Hasegawa and Kodama, 1995)

$$\xi=\varepsilon(x-C_g t),\quad T=\varepsilon^2 t, \tag{6}$$

then when it is substituted into Eq.(5), we obtain

$$\begin{aligned}&L(\psi')+\bar{u}\frac{\partial h'}{\partial x}+\varepsilon\Big[(\bar{u}-C_g)\frac{\partial}{\partial\xi}(\nabla^2\psi'-F\psi')+2\Big(\frac{\partial}{\partial t}+\bar{u}\frac{\partial}{\partial x}\Big)\frac{\partial^2\psi'}{\partial x\partial\xi}+(\beta+F\bar{u})\frac{\partial\psi'}{\partial\xi}\\&+J(\psi',\nabla^2\psi'+h')\Big]+\varepsilon^2\Big[\frac{\partial}{\partial T}(\nabla^2\psi'-F\psi')+2(\bar{u}-C_g)\frac{\partial^3\psi'}{\partial x\partial\xi^2}+\Big(\frac{\partial}{\partial t}+\bar{u}\frac{\partial}{\partial x}\Big)\frac{\partial^2\psi'}{\partial\xi^2}\\&+J\Big(\psi',2\frac{\partial^2\psi'}{\partial x\partial\xi}\Big)+\frac{\partial\psi'}{\partial\xi}\frac{\partial}{\partial y}\nabla^2\psi'-\frac{\partial\psi'}{\partial y}\frac{\partial}{\partial\xi}\nabla^2\psi'\Big]+\varepsilon^3\Big[(\bar{u}-C_g)\frac{\partial^3\psi'}{\partial\xi^3}+2\frac{\partial^3\psi'}{\partial x\partial\xi\partial T}\\&+\frac{\partial\psi'}{\partial\xi}\frac{\partial h'}{\partial y}+J\Big(\psi',\frac{\partial^2\psi'}{\partial\xi^2}\Big)+2\frac{\partial\psi'}{\partial\xi}\frac{\partial^3\psi'}{\partial x\partial y\partial\xi}-2\frac{\partial\psi'}{\partial y}\frac{\partial^3\psi'}{\partial x\partial\xi^2}\Big]+O(\varepsilon^4)=0,\end{aligned} \tag{7}$$

with the boundary conditions that

$$\frac{\partial\psi}{\partial x}=0,\quad \frac{\partial^2\overline{\psi'(y,t,T)}}{\partial y\partial t}=0,\quad \frac{\partial^2\overline{\psi'(y,t,T)}}{\partial y\partial T}=0,\quad y=0,\quad L_y, \tag{8}$$

where $L(\ )=\left(\frac{\partial}{\partial t}+\bar{u}\frac{\partial}{\partial x}\right)[\nabla^2(\ )-F(\ )]+(\beta+F\bar{u})\frac{\partial(\ )}{\partial x}$ is a linear Rossby wave operator.

In Hart (1979), Charney and Devore (1979), Trevisan and Buzzi (1980) the topography was assumed to be a periodic forcing. In this paper because the bottom topography has been assumed to be a wavenumber–two symmetric topography (Charney and Devore, 1979; Li et al., 1986), if the topographic feature is prescribed, the analytical solution to Eq.(7) can be obtained when all the higher order terms larger than the order ε are neglected. However, if all higher order terms are considered, the solution to Eq.(7) should contain small terms. In order to obtain a higher order NLS equation, a new perturbation expansion method proposed by Luo (2000b) is used to solve Eq.(7). Assume that Eq.(7) has the solution of $\psi' = \psi_0 + \varepsilon\psi_{10}$. When ψ_0 is determined from Eq.(7) without the terms equal to or greater than ε, the nonlinear equation for ψ_{10} can be obtained by substituting $\psi' = \psi_0 + \varepsilon\psi_{10}$ into Eq.(7). If the solution of the nonlinear equation for ψ_{10} is assumed to be of the form $\psi_{10} = \psi_1 + \varepsilon\psi_{20}$, then its linear solution ψ_1 can be easily derived when the higher order terms larger than the order ε in this equation are neglected. Similarly, the nonlinear equation for ψ_{20} can also be obtained by substituting $\psi_{10} = \psi_1 + \varepsilon\psi_{20}$ into the nonlinear equation for ψ_{10}. Through a series of the same algebraic operation, the asymptotic solution to Eq.(7) can be derived. Based on this expansion method, a higher order NLS equation including higher order terms is also obtained in such an algebraic operation. It should be pointed out that the advantage of the perturbation expansion method used here can make nonlinear Schrödinger equation include the higher order terms equal to or greater than the order ε, but the traditional perturbation expansion cannot.

In the present paper the prescribed topography is assumed to be of the form

$$h' = h'_0 \exp(ikx)\sin(\frac{m}{2}y) + C_c, \tag{9}$$

where h'_0 is the topographic amplitude, $k = \frac{2}{6.371\cos(\varphi_0)}$ denotes the wavenumber of zonal wavenumber–two, $m = -\frac{2\pi}{L_y}$ is the topographic meridional wavenumber, and C_c denotes the complex conjugate of its preceding term.

Clearly, for the dipole meridional structure, the solution to Eq.(7) can be expressed as

$$\begin{aligned}\psi' = \psi_0 + \varepsilon\psi_1(\xi,T,x,y,t) = A(T,\xi)\varphi_1(y)\exp[i(kx-\omega t)] + \\ h_A h'_0 \exp(ikx)\sin(my/2) + \varepsilon\psi_1 + C_c,\end{aligned} \tag{10}$$

where A is the slowly varying complex amplitude of linear Rossby wave for zonal wavenumber–two, $\varphi_1(y) = \sqrt{\frac{2}{L_y}}\sin(my)$, $h_A = \frac{1}{\frac{\beta}{\bar{u}} - (k^2 + \frac{m^2}{4})}$ and $\omega = \bar{u}k - \frac{(\beta + \bar{u}F)k}{k^2 + m^2 + F}$ is the frequency of linear Rossby wave for zonal wavenumber–two. Note that the second term in the right–hand side of (10) is the standing wave induced by the wavy topography (9).

The substitution of (10) into Eq.(7) yields

$$\begin{aligned}
&L(\psi_1) + i\frac{km}{4}(\frac{3}{4}m^2 h_A + 1)h'_0(\frac{2}{L_y})^{\frac{1}{2}}[A\exp(-i\omega t) - A^*\exp(i\omega t)][3\sin(\frac{3m}{2}y) - \sin(\frac{m}{2}y)] \\
&- i\frac{km}{4}(\frac{3}{4}m^2 h_A + 1)h'_0(\frac{2}{L_y})^{\frac{1}{2}}\exp[i(2kx-\omega t)][\sin(\frac{3m}{2}y) - 3\sin(\frac{m}{2}y)] + \varepsilon[\frac{\partial}{\partial T}(\nabla^2\psi_0 - F\psi_0) \\
&+ 2(\bar{u} - C_g)\frac{\partial^3\psi_0}{\partial x\partial\xi^2} + (\frac{\partial}{\partial t} + \bar{u}\frac{\partial}{\partial x})\frac{\partial^2\psi_0}{\partial\xi^2} + (\bar{u} - C_g)\frac{\partial}{\partial\xi}(\nabla^2\psi_1 - F\psi_1) \\
&+ (\beta + F\bar{u})\frac{\partial\psi_1}{\partial\xi} + J(\psi_0, \nabla^2\psi_1) \\
&+ J(\psi_1, \nabla^2\psi_0 + h') + J(\psi_0, 2\frac{\partial^2\psi_1}{\partial x\partial\xi}) + \frac{\partial\psi_0}{\partial\xi}\frac{\partial}{\partial y}\nabla^2\psi_1 - \frac{\partial\psi_0}{\partial y}\frac{\partial}{\partial\xi}\nabla^2\psi_1] + \varepsilon^2[(\bar{u} - C_g)\frac{\partial^3\psi_0}{\partial\xi^3} \\
&+ 2\frac{\partial^3\psi_0}{\partial x\partial\xi\partial T} + J(\psi_0, \frac{\partial^2\psi_0}{\partial\xi^2}) + \frac{\partial\psi_0}{\partial\xi}\frac{\partial}{\partial y}(2\frac{\partial^2\psi_0}{\partial x\partial\xi}) - \frac{\partial\psi_0}{\partial y}\frac{\partial}{\partial\xi}(2\frac{\partial\psi_0}{\partial x\partial\xi}) + J(\psi_0, 2\frac{\partial^2\psi_1}{\partial x\partial\xi})
\end{aligned}$$

$$+ J(\psi_1, 2\frac{\partial\psi_0}{\partial x\partial\xi}) + \frac{\partial\psi_0}{\partial\xi}\frac{\partial}{\partial y}\nabla^2\psi_1 + \frac{\partial\psi_1}{\partial\xi}\frac{\partial}{\partial y}\nabla^2\psi_0 - \frac{\partial\psi_0}{\partial y}\frac{\partial}{\partial\xi}\nabla^2\psi_1 - \frac{\partial\psi_1}{\partial\xi}\frac{\partial}{\partial\xi}\nabla^2\psi_0 + J(\psi_1, \nabla^2\psi_1)] + O(\varepsilon^3) = 0. \tag{11}$$

After a series of algebraic operation, under the condition $\omega \neq 0$ the solution to Eq.(11) can be expressed as

$$\psi_1 = \psi_{11}(T,\xi,x,y,t) + \psi_{12}(T,\xi,x,y,t) + \psi_{13}(T,\xi,y) + \varepsilon\psi_2, \tag{12}$$

where

$$\psi_{11} = -\frac{km}{4\omega}(\frac{3}{4}m^2 h_A + 1)h'_0(\frac{2}{L_y})^{\frac{1}{2}}[A\exp(-i\omega t) + A^*\exp(i\omega t)] \times \sum_{n=1}^{\infty}\frac{(3a_n - b_n)}{(nm)^2 + F}\cos(nmy), \tag{13}$$

$$\psi_{12} = \frac{km}{4}(\frac{3}{4}m^2 h_A + 1)h'_0(\frac{2}{L_y})^{\frac{1}{2}} A\exp[i(2kx - \omega t)][p_1\sin(\frac{3m}{2}y) - p_2\sin(\frac{m}{2}y)], \tag{14}$$

$$\psi_{13} = -|A|^2\sum_{n=1}^{\infty} q_n g_n \cos(n + \frac{1}{2})my, \tag{15}$$

and ψ_2 satisfies the equation

$$\begin{aligned} &L(\psi_2) + \frac{\partial}{\partial t}(\nabla^2\psi_0 - F\psi_0) + 2(\bar{u} - C_g)\frac{\partial^3\psi_0}{\partial x\partial\xi^2} + (\frac{\partial}{\partial t} + \bar{u}\frac{\partial}{\partial x})\frac{\partial^2\psi_0}{\partial\xi^2} + J(\psi_1, \nabla^2\psi_0 + h') \\ &+ J(\psi_0, \nabla^2\psi_1) + J(\psi_0, 2\frac{\partial^2\psi_0}{\partial x\partial\xi}) + \frac{\partial\psi_0}{\partial\xi}\frac{\partial}{\partial y}(\nabla^2\psi_0 h') - \frac{\partial\psi_0}{\partial y}\frac{\partial}{\partial\xi}(\nabla^2\psi_0 + h') \\ &+ \varepsilon[(\bar{u} - C_g)\frac{\partial^3\psi_0}{\partial\xi^3} + 2\frac{\partial^3\psi_0}{\partial x\partial\xi\partial T} + J(\psi_0, \frac{\partial^2\psi_0}{\partial\xi^2}) + \frac{\partial\psi_0}{\partial\xi}\frac{\partial}{\partial y}(2\frac{\partial^2\psi_0}{\partial x\partial\xi}) - \frac{\partial\psi_0}{\partial y}\frac{\partial}{\partial\xi}(2\frac{\partial^2\psi_0}{\partial x\partial\xi}) \\ &+ J(\psi_0, 2\frac{\partial^2\psi_1}{\partial x\partial\xi}) + J(\psi_1, 2\frac{\partial^2\psi_0}{\partial x\partial\xi}) + \frac{\partial\psi_0}{\partial\xi}\frac{\partial}{\partial y}\nabla^2\psi_1 + \frac{\partial\psi_1}{\partial\xi}\frac{\partial}{\partial y}(\nabla^2\psi_0 + h') \\ &- \frac{\partial\psi_0}{\partial y}\frac{\partial}{\partial\xi}\nabla^2\psi_1 - \frac{\partial\psi_1}{\partial y}\frac{\partial}{\partial\xi}\nabla^2\psi_0] + O(\varepsilon^2) = 0, \end{aligned} \tag{16}$$

where the coefficients of (13)–(15) are given in Appendix A.

Note that if $A=0$ is allowed, (10) can be reduced to the topographically induced stationary wave obtained by Tung and Lindzen (1979). When $\bar{u} = \beta/(k^2 + m^2/4)$, this wave is a resonant topographically forced wave. This resonance is the so–called CDV–type monopole resonance (Charney and Devore, 1979), which requires strong unrealistic basic westerly wind. However, because the Rossby wave studied here has a dipole meridional structure, the CDV–type monopole resonance does not occur when ω is very small, but the dipole near–resonance is possible. This near–resonance is the so–called LG–type dipole near–resonance (Legras and Ghil, 1985; Luo, 1997b), which requires weaker, more realistic background westerly wind (Luo, 1997b). When LG–type dipole near–resonance occurs, the CDV–type monopole resonance or near–resonance can be avoided. If $L_y=5$ (5000 km in the dimensional form, which is approximate to the meridional scale of blockings) is allowed, then $\omega=0.0183\sim0.0648$ for $\bar{u}=0.75\sim0.88$ at 55°N. In this case, we may assume $\omega=\varepsilon^2\Omega$. As a result, the envelope Rossby soliton studied is almost stationary and also called a near–resonant dipole soliton. For this reason, in this paper our attention is focused on studying near–resonant soliton.

Substituting (9), (10) and (12) into (16), the vanishing condition of $\exp[i(kx-\omega t)]$ requires that

$$i\frac{\partial A}{\partial T}=\lambda\frac{\partial^2 A}{\partial \xi^2}+\delta|A|^2A+Sh_0'^2A+Rh_0'^2[A^*\exp(2i\Omega T)+A]=i\varepsilon\{R_1\frac{\partial^3 A}{\partial \xi^3}+R_2\frac{\partial(|A|^2A)}{\partial \xi}+R_3A\frac{\partial|A|^2}{\partial \xi}\;R_4h_0'^2\frac{\partial A}{\partial \xi}+R_5h_0'^2[\frac{\partial A^*}{\partial \xi}\exp(2i\Omega T)+\frac{\partial A}{\partial \xi}]\}+O(\varepsilon^2)=0, \quad (17)$$

where $\Omega=\frac{\omega}{\varepsilon^2}$, and the coefficients of Eq.(17) are given in Appendix B.

It should be pointed out that although Eq.(17) contains the term $\omega t(\omega t=\Omega T)$, it only causes the slow variation of the envelope amplitude A. This assumption is crudely acceptable for a very small ω. However, if ω is larger, Eq.(17) is invalid. This problem is beyond the scope of the present paper.

Under the condition $\lambda>0$ and $\delta>0$, if the transformations $A=B\exp(i\Omega T)/\sqrt{\delta}$ and $\xi=(2\lambda)^{\frac{1}{2}}X$ are made, then Eq.(17) can be rewritten as

$$i\frac{\partial B}{\partial T}+\frac{1}{2}\frac{\partial^2 B}{\partial X^2}+|B|^2B=P(B)=-\alpha_0B-\nu_0B^*+i\varepsilon[\gamma_1\frac{\partial^3 B}{\partial X^3}+\gamma_2\frac{\partial(|B|^2B)}{\partial X}+\gamma_3B\frac{\partial|B|^2}{\partial X}+\gamma_4\frac{\partial B}{\partial X}+\gamma_5\frac{\partial B^*}{\partial X}], \quad (18)$$

where $\alpha_0=(S+R)h_0'^2-\Omega$, $\nu_0=Rh_0'^2$, $\gamma_1=(2\lambda)^{-\frac{3}{2}}R_1$, $\gamma_2=\frac{R_2}{\delta}(2\lambda)^{-\frac{1}{2}}$, $\gamma_3=\frac{R_3}{\delta}(2\lambda)^{-\frac{1}{2}}$, $\gamma_4=(2\lambda)^{-\frac{1}{2}}(R_4+R_5)h_0'^2$ and $\gamma_5=(2\lambda)^{-\frac{1}{2}}R_5h_0'^2$.

Eq.(18) is a new parametrically excited HNLS equation, which has not been yet obtained by the previous investigators. This equation describes the interaction between slowly moving envelope Rossby soliton for zonal wavenumber–two and wavenumber–two topography under the LG–type dipole near–resonance. When both the topographic forcing and higher order terms ($\gamma_1,\gamma_2,\gamma_3,\gamma_4$, and γ_5) are neglected, this equation reduces to the formal nonlinear Schrödinger (NLS) equation governed by the envelope amplitude of nonlinear Rossby waves without forcing in the geophysical fluid derived by Benney (1979), Yamagata (1980), Boyd(1983) and Luo (1991). Neglecting the terms $O(\varepsilon)$ in Eq.(18), it is identical to the parametrically excited NLS equation obtained by Miles (1984) for parametrically excited solitary wave in surface water waves and then by Luo (1997a, 1999) for parametrically forced envelope Rossby solitons. For case without forcing ($h'_0=0$), Eq.(18) reduces to the HNLS equation obtained by Hasegawa and Kodama (1995) in the optical fibers and by Luo (2000b) for weakly nonlinear Rossby waves. Naturally, Eq.(18) may be considered as an extension of the NLS equation obtained by Miles (1984) and Luo(1997a,1999). Here, if $F=1.0$ and $L_y=5.0$ are allowed, then both $\lambda>0$ and $\delta>0$ always exist in the mid–high latitude regions. In this case, Eq.(18) without both forcing and higher order terms possesses an envelope soliton solution (Yamagata, 1980). In this paper, in order to gain a better understanding the interaction of slowly moving envelope Rossby soliton with a wavenumber–two topography, we will present the numerical solution of Eq.(18) in the following section.

3. The interaction of slowly moving planetary–scale envelope Rossby soliton with a wavenumber–two topography

We plot the horizontal distribution of wavenumber–two topography before the interaction of slowly moving planetary–scale envelope Rossby soliton with wavenumber–two topography is investigated. If one defines $h_0 = \varepsilon h'_0$, then the symmetric wavenumber–two topography can be expressed as

$$h = 2h_0 \cos(kx)\sin(my / 2). \tag{19}$$

In (19), because $m / 2 = -\pi / L_y$, the bottom topography exhibits a monopole structure in the meridional direction. Figure 1 shows the horizontal distribution of wavenumber–two topography at 55°N for the parameters $L_y = 5.0$ and $h_0 = 0.5$.

It is found that the height of the wavenumber–two topography is near 1.0 km. This horizontal distribution represents the actual topography (the two oceans and two continents), and has the same form as that given by Charney and DeVore (1979) and Li et al. (1986). In this figure, the positive regions denote the topographic ridges (the two continents), while the negative regions represent the topographic troughs (the two oceans).

In this paper, in order to investigate the propagation of planetary–scale envelope Rossby soliton over a wavenumber–two topography, the finite difference scheme used by Taha and Ablowitz (1984) will be applied in solving Eq.(18). The incipient envelope soliton solution to Eq.(18) is assumed to be of the form

$$B(X,0) = B_0 \operatorname{sech}(B_0 X), \tag{20}$$

where B_0 is the value of $B(X,0)$ at $X = 0$.

We choose $B_0 = 0.6\sqrt{\delta} / \varepsilon$, $\varepsilon h'_0 = 0.5$, $\varepsilon = 0.34$, and $\bar{u} = 0.83$. If one defines $M = |B(X,T)|$, then the contour plots of $M = |B(X,T)|$, at 55°N are plotted in Fig. 2 in the soliton–topography interaction.

We can see from Fig. 2a that when the higher order terms are neglected, the near–resonantly forced envelope soliton does not propagate in the moving framework X even though it can be amplified and can exhibit an amplitude oscillation. Only in the two flanks of the peak of the large–amplitude soliton a series of small–amplitude wave trains can be observed. However, it is not

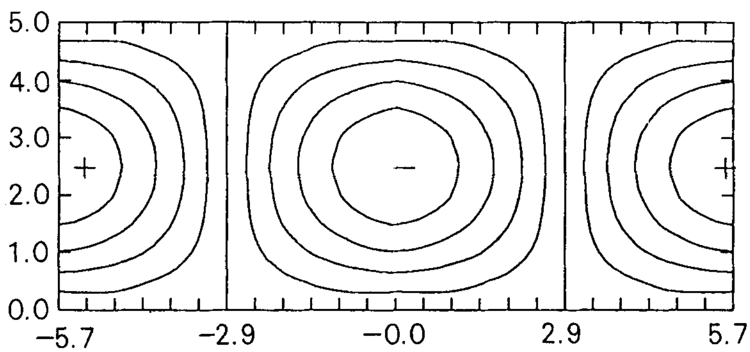

Fig. 1. The horizontal distribution of wavenumber–two topography at 55°N for the chosen parameters $L_y = 5$ and $h_0 = 0.5$. Contour interval 0.2.

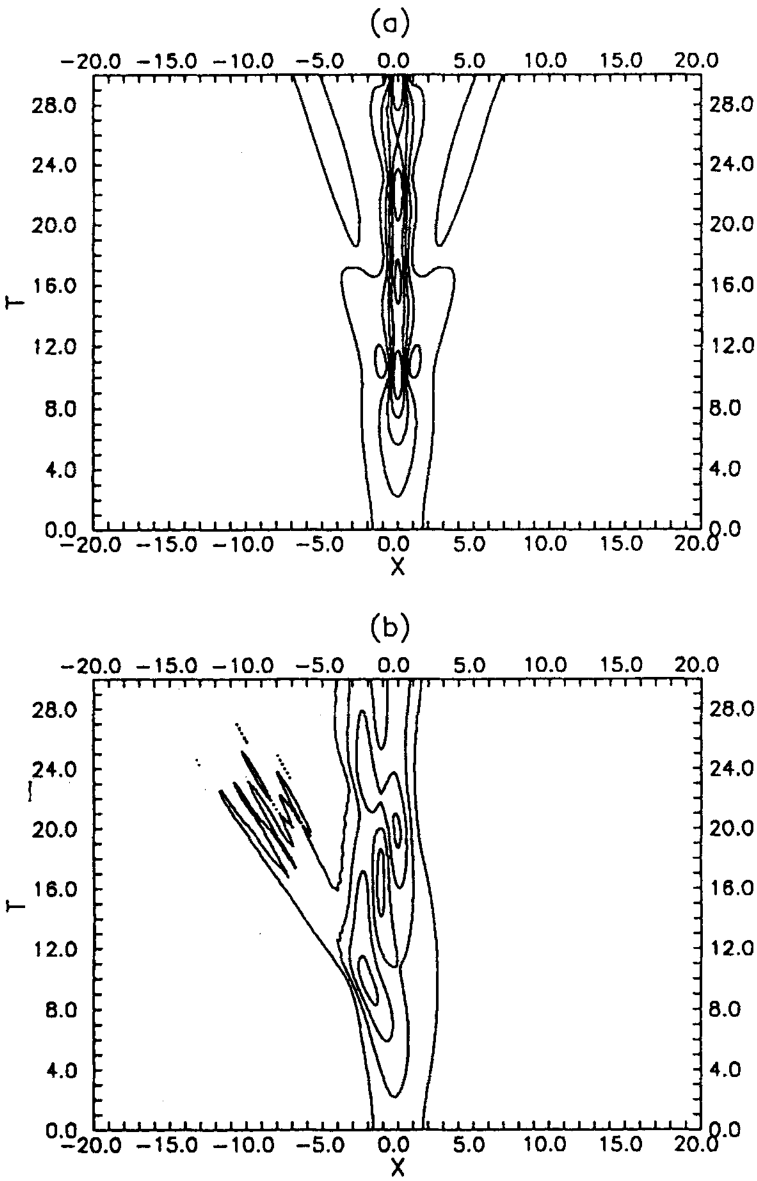

Fig. 2. The contour plot of $|B(X,T)|$ in the (X,T)–plane for parameters $\varepsilon h'_0 = 0.5$, $\varepsilon = 0.34$, $B_0 = 0.6\sqrt{\delta} / \varepsilon$, and $\bar{u} = 0.83$: (a) without higher order terms; (b) with higher order terms. Contour interval 0.4.

difficult to observe in Fig.2b that in the amplifying process of planetary–scale soliton by a wavenumber–two topography, the large–amplitude soliton peak propagates westward and a series of small–amplitude wave trains that propagate westward are excited. Interestingly, the large–amplitude soliton begins to propagate eastward after it reaches a certain location. The propagation of the large–amplitude soliton peak is not clear in the moving framework X after it reaches $X=0$. In order to show the propagation behaviour of planetary–scale envelope Rossby soliton, we plot the distribution of $M = |B(X,T)|$ only dependent on X for different T in Fig.3. We find that at $T=0$ the maximum amplitude of $|B(X,T)|$ for $X=0$ is near 0.72. However, at $T=3.0$ it becomes

1.75 through the near–resonant forcing of wavenumber–two topography. The topographically forced soliton is found to possess a deformation and to have a westward propagation. After $T=3.0$ the soliton begins to break up and its maximum amplitude is also decreased. Further, at $T=6.0$ this soliton begins to propagate eastward, and at $T=7.0$ its maximum amplitude is located in $X=0$ and near 1.7. Afterwards, this soliton propagates westward again and its maximum amplitude is increased. In the whole process, a series of small–amplitude wave trains that propagate westward are excited gradually. Therefore, we conclude that the higher order terms has an important influence on the interaction between slowly moving planetary–scale envelope Rossby soliton and a wavenumber–two topography.

Under the same condition as in Fig.2b, Fig. 4 shows the instantaneous total streamfunction fields (the sum of the streamfunction fields of planetary–scale dipole soliton and topographically induced standing wave) of slowly moving planetary–scale envelope Rossby soliton with an initial amplitude $B_0 = 0.6\sqrt{\delta} / \varepsilon$, at 55°N, interacting with a wavenumber–two topography for the same parameters as in Fig.2. It is easy to find that in the soliton–topography interaction process, the incipient small–amplitude slowly moving envelope Rossby soliton situated in $x=0$ can be amplified. At day 0 only a weak blocking high, usually called " high–index" flow, appears at $x=0$ because the amplitude of the dipole soliton is too small. However, this planetary–scale soliton will be gradually amplified through the near–resonant forcing of wavenumber–two topography. For example, at day 27, a blocking high is formed. Accompanied by the further amplifying of the soliton amplitude, this blocking high will be further intensified and developed into an omega–type blocking (see the plots during the period from day 33 to 57). After day 63, this blocking high begins to weaken. In the whole process, the blocking high is almost located in the topographic trough. This may be the reason why most of blocking high occurs in the two oceans (Treidl et al., 1981).We conclude that the observed blocking highs may be associated with the near–resonant forcing of a wavenumber–two topography. However, the forcing of synoptic–scale eddies was also found to play a rather important role in the initiation and maintenance of dipole blockings (Shutts, 1983; Holopainen and Foretlius, 1987). Thus, as a completely theoretical model of blocking the forcing of synoptic–scale eddies should be included. This problem will be further investigated elsewhere. At 60°N, the instantaneous total streamfunction fields of slowly moving planetary–scale envelope Rossby soliton interacting with a wavenumber–two topography for $\varepsilon h'_0 = 0.5$, $\varepsilon = 0.34$, $B_0 = 0.4\sqrt{\delta} / \varepsilon$, and $\bar{u} = 0.75$ are depicted in Fig. 5.

It can be seen from Fig.5 that in the higher–latitude region, the dipole blocking can be excited through the near–resonant interaction between slowly moving envelope Rossby soliton and wavenumber–two topography. This figure can describe the life cycle of dipole blocking. Thus, the near–resonant interaction between slowly moving envelope Rossby soliton and wavenumber–two topography can produce the dipole blocking in the higher–latitude region.

Egger (1978) showed that blocking could be produced through the nonlinear interaction among forced and slowly moving free waves. Legras and Ghil (1985) pointed out that the LG–type dipole resonance has a more complicated structure than the CDV–type monopole resonance. For a prescribed monopole topography, in a complicated truncated spectral model they found that under the LG–type dipole resonance condition, blocking high can occur in the upstream of the topographic ridge. This also confirms from another aspect that our result is reasonable. Unfortunately, our model cannot model all observed blocking patterns because other physical factors have been ignored. These problems deserve further study. On the other hand, it should be pointed out that the choice of

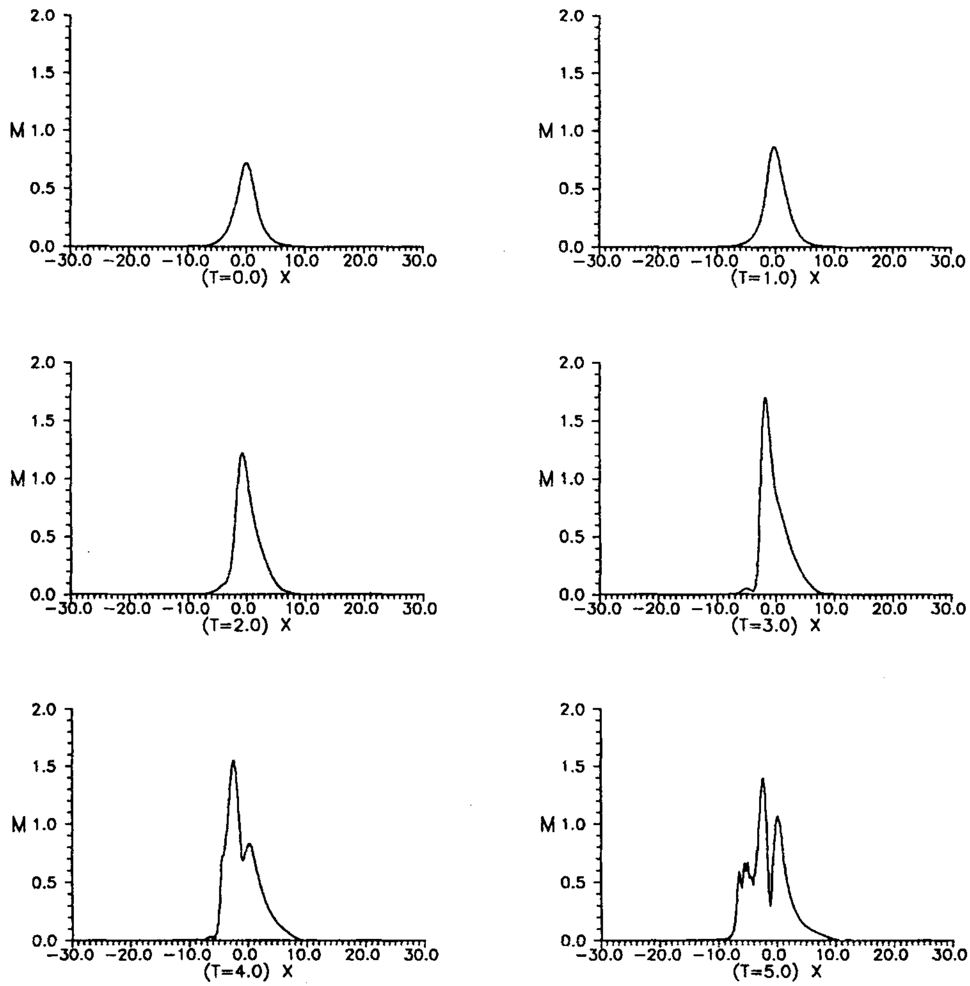

the perturbation parameter does not strongly influence our results. This problem is easily tested by choosing $\varepsilon = 0.24$ (figures omitted). In the previous studies the topography is found to play a significant role in the onset of blockings (Egger, 1978; Tung and Lindzen, 1979; Charney and DeVore, 1979). A very interesting problem is why the wavenumber–two topography can reinforce and maintain blocking high (Charney and Devore, 1979). This problem is not answered completely so far. In the following section, this problem will be investigated by solving Eq.(18) in terms of the soliton perturbation theory (Kaup and Newell, 1978; Abdullaev, 1989; Hasegawa and Kodama, 1995).

4. Why can the wavenumber–two topography reinforce and maintain blocking?

It is not difficult to see from Fig.3 that in the soliton–topography interaction, the breakdown of the soliton is not remarkable. In this case, in order to explore the underlying physical mechanism of blocking high, the solution to Eq.(18) is still assumed to be an envelope soliton solution. This assumption is approximately acceptable before the soliton breaks up completely. In the present paper, the topographic forcing and higher order terms in Eq.(18) are regarded as a perturbation of the formal NLS equation. On this basis, the perturbed inverse scattering transform (IST) method can be

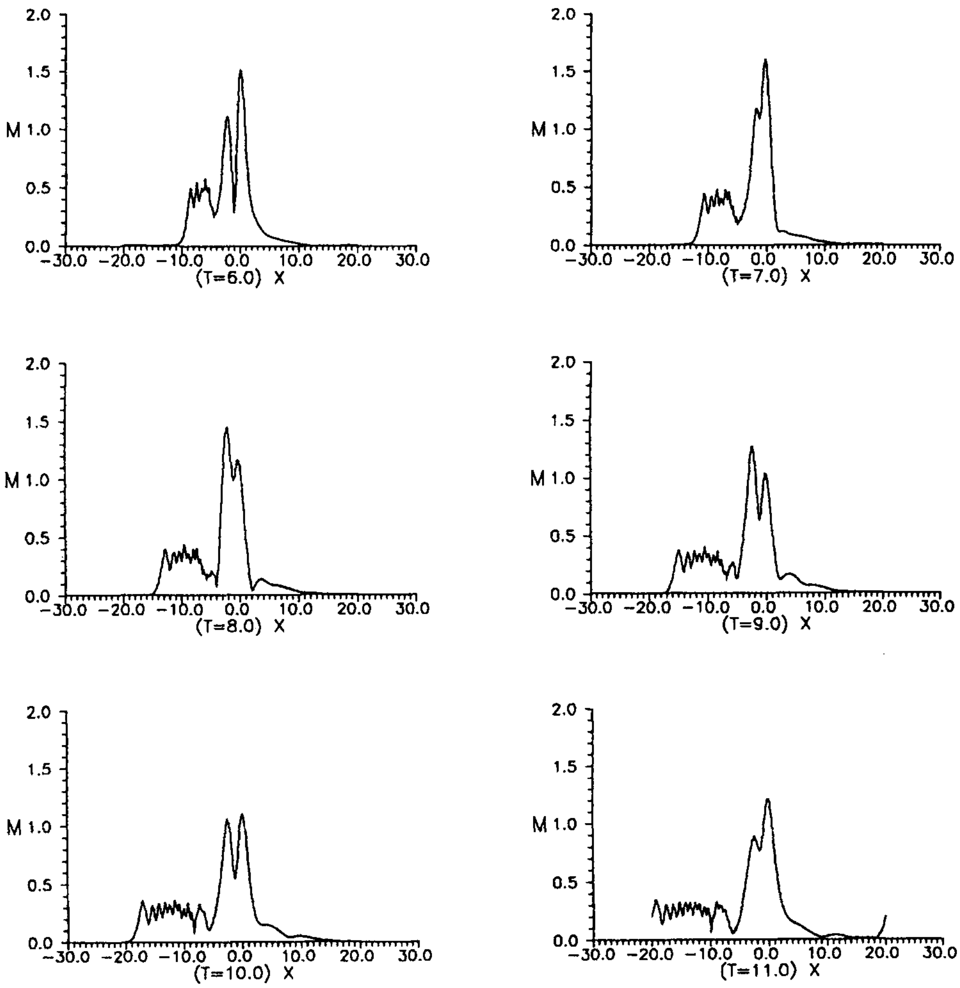

Fig. 3. The evolution of $|B(X,T)|$ for different T. The chosen parameters are the same as in Fig. 2b.

also used to solve Eq.(18) even when the perturbation term $P(B)$ is not small (Chen and Wei, 1994; Hasegawa and Kodama, 1995).

In the interaction between slowly moving dipole envelope Rossby soliton and wavenumber–two topography, the soliton parameters such as amplitude, group velocity and phase can be assumed to be slow time–variation. In this case, in order to investigate the evolution of the fundamental NLS soliton under the topographic forcing and higher order terms, the solution of Eq.(18) can be assumed to have the general form of the soliton solution depending on T, that is,

$$B(X,T)= B_0(T)\mathrm{sech}\{B_0(T)[X+\kappa(T)]\}\exp[i\theta(T)], \tag{21}$$

where $B_0(T)$, $\kappa(T)$ and $\theta(T)$ are the amplitude, group velocity and phase of the soliton.

The evolution equations for these soliton parameters can be obtained with the help of the inverse scattering transform (IST) method of the soliton perturbation theory (Kaup and Newell, 1978; Kivshar and Malomed, 1989; Abdullaev, 1989; Hasegawa and Kodama, 1995). If one defines $\theta(\varepsilon^2 t)$

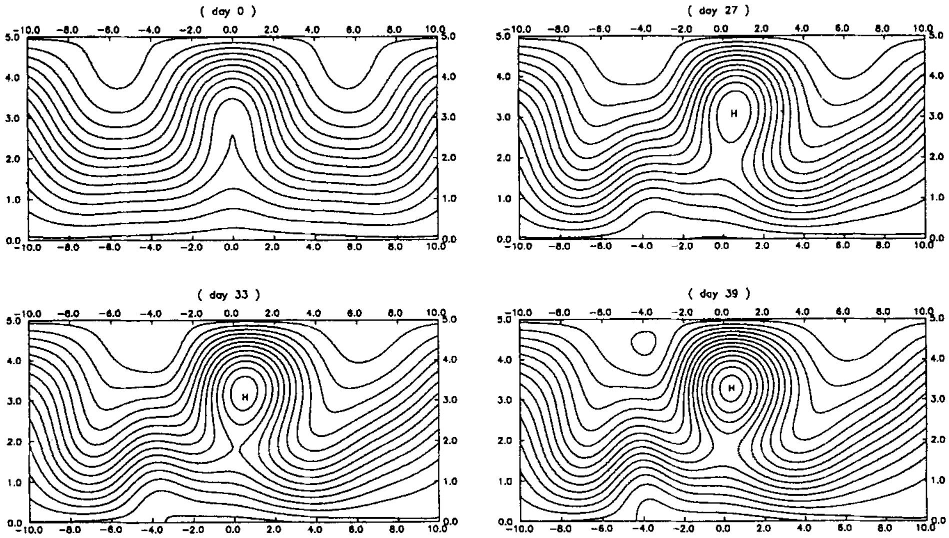

$= P(t)$, $\varepsilon B_0(\varepsilon^2 t) = \sqrt{\delta}\, M(t)$ and $Z(t) = \kappa(\varepsilon^2 t)\sqrt{2\lambda}\,/\,\varepsilon$, then these soliton parameter equations can be easily obtained as

$$\frac{dM}{dt} = 2\nu M \sin 2P, \tag{22}$$

$$\frac{dZ}{dt} = -M^2\left(\frac{\delta}{2\lambda}R_1 - R_2 - \frac{2}{3}R_3\right) + (R_4 + R_5)h_0^2 + R_5 h_0^2 \cos 2P, \tag{23}$$

$$\frac{dP}{dt} = \frac{\delta}{2}M^2 + \alpha + \nu\cos 2P, \tag{24}$$

where $\alpha = \varepsilon^2\alpha_3 = (S + R)h_0^2 - \omega$, $\nu = \varepsilon^2 \nu_0 = R h_0^2$ and $h_0 = \varepsilon h'_0$.

Eqs.(22)–(24) describe the deformation of a slowly moving planetary–scale dipole envelope Rossby soliton during the interaction with a wavenumber–two topography in terms of its amplitude, group velocity and phase including the higher order terms. In these equations, it can be found that the equations for variables $M(t)$ and $P(t)$ are independent of variable $Z(t)$, but the equation for $Z(t)$ contains both variables $M(t)$ and $P(t)$. Thus, it can be concluded that the $Z(t)$ equation has no stationary solution even if the equations for variables $M(t)$ and $P(t)$ have stationary state solutions. It can be proved from Eqs.(22)–(24) that stable, slowly moving dipole envelope Rossby soliton can exist over a wavenumber–two topography.

Using (4),(10) and (12), the total streamfunction of planetary–scale dipole envelope Rossby soliton interacting with wavenumber–two topography can be expressed as

$$\psi \approx -\bar{u}y + \varepsilon\psi_0 + \varepsilon^2\psi_1 + O(\varepsilon^3) = -\bar{u}y + 2\left(\frac{2}{L_y}\right)^{\frac{1}{2}} M(t)\operatorname{sech}\left\{\left(\frac{\delta}{2\lambda}\right)^{\frac{1}{2}} M(t)[x - Cgt + Z(t)]\right\} \times$$

$$\cos[kx + P(t)]\sin(my) + 2h_A h_0 \cos(kx)\sin\left(\frac{m}{2}y\right) - M(t)^2 \operatorname{sech}^2\left\{\sqrt{\frac{\delta}{2\lambda}}\, M(t)[x - Cgt + Z(t)]\right\} -$$

$$\frac{km}{2\omega}\left(\frac{3}{4}h_A^2 m^2 + 1\right)h_0 \sqrt{\frac{2}{L_y}}\, M(t)\operatorname{sech}\left\{\sqrt{\frac{\delta}{2\lambda}}\, M(t)[x - Cgt + Z(t)]\right\}$$

$$\cos[P(t)]\cos[P(t)]\sum_{n=1}^{\infty}\frac{(3a_n - b_n)}{(nm)^2 + F}\cos(nmy)$$

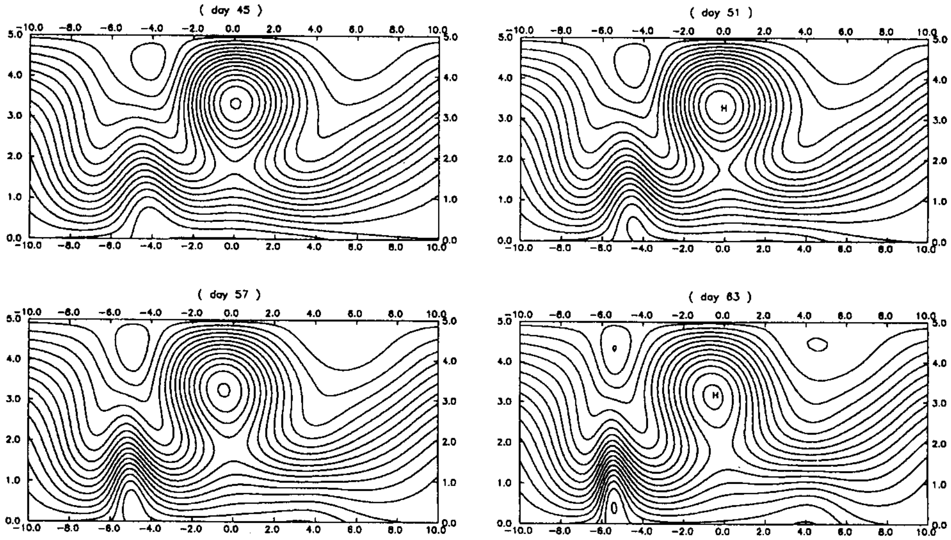

Fig. 4. The instantaneous total streamfunction field of envelope Rossby soliton with higher order terms interacting with the wavenumber–two topography at 55°N, at 3 days intervals, for the same parameters as in Fig.2b. Contour interval 0.3.

$$+\frac{km}{2}(\frac{3}{4}m^2h_A+1)h_0\sqrt{\frac{2}{L_y}}M(t)\text{sech}\{\sqrt{\frac{\delta}{2\lambda}}M(t)[x-Cgt+Z(t)]\}\cos[2kx+P(t)]$$
$$\times[p_1\sin(\frac{3m}{2}y)-p_2\sin(\frac{m}{2}y)]. \tag{25}$$

In (25), the second term denotes the streamfunction of the slowly moving dipole envelope Rossby soliton, and the third term represents the streamfunction of the topographically induced stationary wave having a monopole meridional structure. It is not difficult to find that if $M(t)=0$ is chosen, (25) is identical to the expression of the topographically induced standing wave obtained by Tung and Lindzen (1979). For a prescribed background westerly wind, when $h_A<0(\bar{u}-\bar{u}_c<0,\ \bar{u}_c=\beta/(k^2+m^2/4)$ is satisfied, a high pressure appears in the topographic trough and a low pressure appears in the topographic ridge because of $m<0$. Contrarily, when $h_A>0(\bar{u}-\bar{u}_c>0)$ holds, a low pressure trough is formed in the topographic trough. Generally speaking, the uniform basic flow that satisfies the LG–type dipole near–resonance can make $\bar{u}_b<<\bar{u}_c$ and cause a small $\bar{u}-\bar{u}_b(\bar{u}_b=\beta/(k^2+m^2))$. In this case, $h_A<0$ is easily satisfied. For this case, a high pres-. sure ridge may appear in the topographic trough. On the other hand, although planetary–scale dipole envelope Rossby soliton studied here possesses a dipole meridional structure, its total streamfunction does not exhibit certainly a dipole structure. This is because the total streamfunction field of the topographically forced dipole envelope Rossby soliton is dependent on the relative magnitude of the amplitude itself and the amplitude of the topographically forced stationary wave.

Based on (25), we can define $Cgm=Cg-dZ/dt$ and $Cpm(t)=-dP/dt$ as the group velocity and phase speed of topographically forced planetary–scale soliton, respectively. In addition, we may define $Cgp=Cgm-Cpm$ as a measure of dispersion. When Cgp tends to be zero, the planetary–scale envelope soliton gradually becomes a non–dispersive system. If the higher order terms for the order $O(\varepsilon)$ are neglected, then the soliton group velocity is independent of

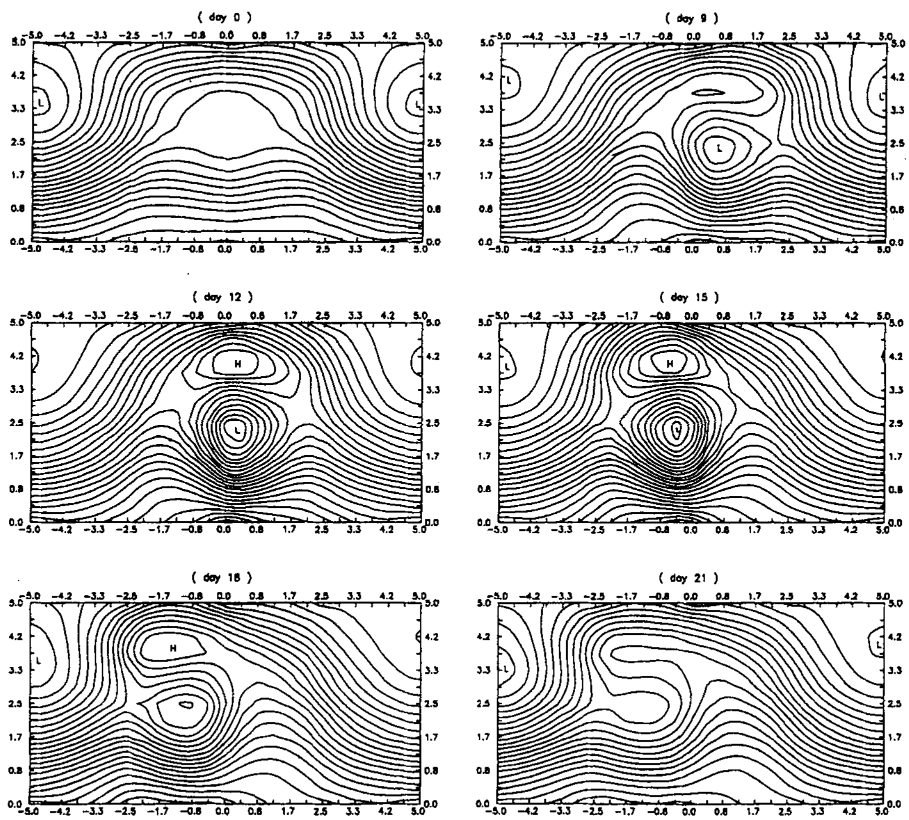

Fig. 5. The instantaneous total streamfunction field of envelope Rossby soliton with higher order terms interacting with the wavenumber–two topography at 60°N, at 3 days intervals, for the same parameters $\varepsilon h'_0 = 0.5$, $\varepsilon = 0.34$, $B_0 = 0.4\sqrt{\delta} / \varepsilon$, and $\bar{u} = 0.75$. Contour interval 0.2.

the topographic feature, but both its amplitude and phase speed depend strongly on the topographic amplitude. However, once the higher order terms are included, the wavenumber–two topography will affect directly the group velocity of the planetary–scale soliton. On the other hand, because both R_4 and R_5 contain the term h_A, the influence of wavenumber–two topography on the soliton group velocity (Cgm) is also dependent on the setting of the near–resonant uniform westerly wind.

As $M(t)$ increases from small to large value, the soliton is amplified by the topography. If Cgp tends to be zero, the planetary–scale envelope soliton can become a weak dispersion even non–dispersion system through the near–resonant forcing of wavenumber–two topography. Thus, if the numerical solutions of Eqs.(22)–(24) can be obtained, the physical mechanism of blocking high produced by a wavenumber–two topography can be understood. In this section, we give the numerical results of Eqs.(22)–(24).

Here, in order to emphasize the role of wavenumber–two topography, as a simplest example we consider a small amplitude envelope Rossby soliton as an incipient soliton. Without the loss of generality we choose the initial data $M(0) = 0.6$, $Z(0) = 0.0$, and $P(0) = 0.0$ at 55°N. The fourth–order Rung–Kutta method is applied to solve Eq.(22)–(24) for parameters $h_0 = 0.5$ and $\bar{u} = 0.83$, and the numerical solutions of $M(t)$, Cgm, Cpm, and Cgp are shown in Fig. 6.

Figure 6 shows the evolution of the parameters $M(t)$, Cgm, Cpm and Cgp in the interaction of slowly moving planetary–scale dipole soliton with a wavenumber–two topography at 55°N. It

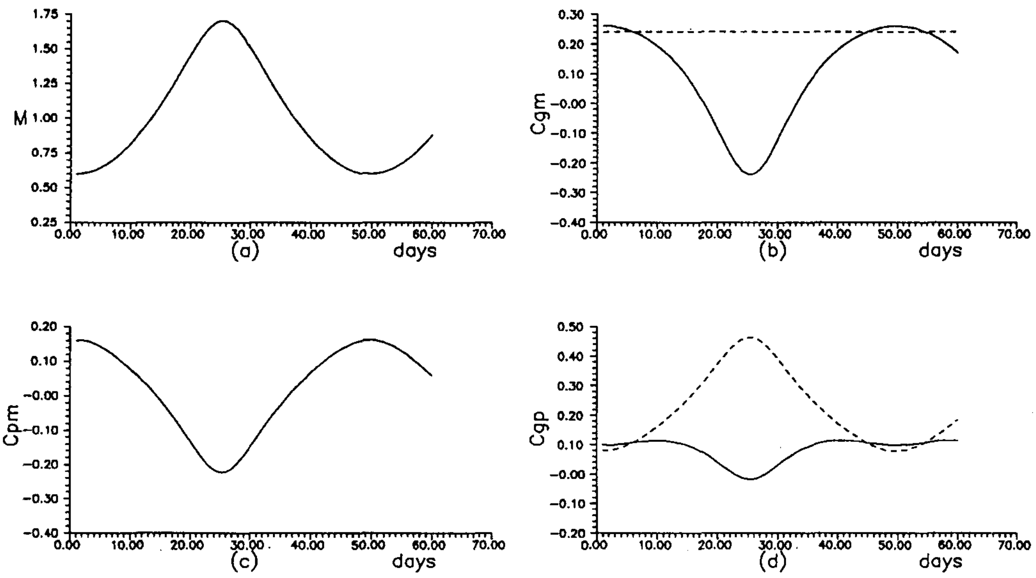

Fig. 6. Time evolution of $M(t)$, Cgm, Cpm, and Cgp during the interaction of slowly moving planetary–scale envelope soliton with wavenumber–two topography at 55°N for parameters $h_0 = 0.5$ and $\bar{u} = 0.83$. The dashed curve represents the case without higher order terms, while the solid curve represents the case with higher order terms. Both $M(t)$ and Cpm are the same for the two cases.

can be noted from this figure that for $\bar{u} = 0.83$, as an incipient small–amplitude planetary–scale soliton, located in the topographic trough, it interacts with a wavenumber–two topography. The soliton amplitude $M(t)$ can increase from 0.6 at day 0 to 1.75 at day 26, and then recover its initial amplitude at day 50. Afterwards, a new oscillation cycle with the same period reappears. In the total process, we note that the higher order terms can decrease the soliton group velocity, but does not influence both the soliton amplitude and the phase speed. On the other hand, it can be found that under the condition with the higher order terms, Cgp tends to be zero even negative in the amplifying process of planetary–scale soliton. In this case, the soliton system has a transfer from dispersion to non–dispersion. This shows that the higher order terms favor the maintenance of blocking high by wavenumber–two topography. This point is easily explained. This is because the inclusion of the higher order terms seems to further emphasize the role of stronger nonlinearity in the establishment of blocking high. In particular, when the nonlinearity becomes so strong that the wave amplitude equation satisfies the KdV equation, the blocking system will become a non–dispersive wave. Thus, under the condition with the higher order terms the blocking system can maintain easily. In other words, the blocking high will become a weak dispersion even non–dispersion system during the stages of its onset and maintenance, but during its decay stage the blocking high will become a dispersion system. To some extent, the results obtained in Fig.6 can explain why the wavenumber–two topography can reinforce and maintain blocking high. Using (25) we can also obtain a blocking structure similar to Fig.4 (figures omitted). The onset, maintenance and decay of dipole blocking in higher latitudes can be similarly explained in terms of the numerical solutions of $M(t)$, Cgm, Cpm, and Cgp at 66°N similar to Fig.6 (figures omitted).

5. Conclusion and discussions

In this paper, a new parametrically excited higher order nonlinear Schrödinger equation is proposed to investigate the near–resonant interaction between slowly moving planetary–scale envelope Rossby soliton and wavenumber–two topography. It is found that when the background westerly wind is under the LG–type dipole near–resonance (Legras and Ghil, 1985; Luo, 1997b), planetary–scale envelope Rossby soliton can be topographically amplified and captured. The role of the higher order terms can cause a transfer of soliton–block from dispersion to weak dispersion even non–dispersion. In addition, a series of small–amplitude wave trains that propagate westward can be excited in this interaction process. There is a similarity between the topographically amplified, captured dipole envelope Rossby soliton and observed blockings. Thus, the topographically amplified, captured dipole envelope Rossby soliton seems to be able to be considered as a model of the onset, maintenance and decay of regional blocking.

Several important questions remain to be examined. First, the direct comparison of these results with the observed blocking and the numerical result of the barotropic model should be made. Also, it is interesting to see whether our topographically amplified planetary–scale envelope Rossby soliton is in detail consistent with the observed transience of blocking. Second, the topographically forced planetary–scale envelope soliton model studied here should contain more physical processes such as baroclinicity, land–sea differential heating and so on. We plan to continue this study with a two–level baroclinic model. On the other hand, a comparison with observational fact should be made. These problems are under current study.

REFERENCES

Abdullaev, F. Kh., 1989: Dynamical chaos of solitons and nonlinear periodic waves. *Phys. Rep.*, **216**, 1–78.

Benney, D. J., 1979: Large amplitude Rossby waves. *Stud. Appl. Math.*, **60**, 1–10.

Boyd, J. P., 1983: Equatorial solitary waves, Part III: Envelope Rossby solitons. *J. Phys. Oceanogr.*, **10**, 1699–1717.

Charney, J. G., and J. G. DeVore, 1979: Multiple flow equilibria in the atmosphere and blocking. *J. Atmos. Sci.*, **35**, 1205–1216.

Chen, X. N., and R. J. Wei, 1994: Dynamic behaviour of a non–propagating soliton under a periodically modulated oscillation. *J. Fluid Mech.*, **259**, 291–303.

Egger, J., 1978: Dynamics of blocking high. *J. Atmos. Sci.*, **35**, 1788–1801.

Hart J.E., 1979: Barotropic quasi–geostrophic flow over an isotropic mountains. *J. Atmos. Sci.*, **36**, 1736–1746.

Hasegawa, A., and Y. Kodama, 1995: *Solitons in Optical Communication*, Clarendon Press, Oxford, 320pp.

Holopainen, E., and C. Fortelius, 1987: High–frequency transient eddies and blocking. *J. Atmos. Sci.*, **44**, 1632–1645.

Kivshar, Y. S., and B. A. Malomed, 1989: Dynamics of solitons in nearly integrable systems. *Rev. Mod. Phys.*, **61(4)**, 763–915.

Kaup, D. J., and A. C. Newell, 1978: Solitons as particles, oscillators, and in slowly changing media: a singular perturbation theory. *Proc. R. Soc. Lond. A.*, **361**, 413–446.

Legras, B., and M. Ghil, 1985: Persistent anomalies, blocking, and variations in atmospheric predictability. *J. Atmos. Sci.*, **42**, 433–471.

Li, G. Q., R. Kung, and R. Pfeffer, 1986: An experimental study of baroclinic flows with and without two–wave bottom topography. *J. Atmos. Sci.*, **43**, 2585–2599.

Luo, D., 1991: Nonlinear Schrödinger equation in the rotational barotropic atmosphere and atmospheric blocking. *Acta Meteorologica Sinica*, **5**, 587–596.

Luo, D., 1997a: Parametrically forced envelope Rossby soliton: Soliton–oscillation. *Geophys. Astrophys. Fluid Dyn.*, **85**, 1–29.

Luo, D., 1997b: Low–frequency finite–amplitude oscillations in a near resonant topographically forced barotropic fluid. *Dyn. Atmos. Oceans*, **26**, 53–72.

Luo, D., 1999: Near resonant topographically forced envelope Rossby solitons in a barotropic flow. *Geophys. Astrophys. Fluid Dyn.*, **90**, 161–188.

Luo, D., 2000a: Planetary–scale baroclinic envelope Rossby solitons in a two–layer model and their interaction with synoptic–scale eddies. *Dyn. Atmos. Oceans*, **32**, 27–74.

Luo, D., 2000b: Derivation of a higher order nonlinear Schrödinger equation for weakly nonlinear Rossby waves. *Wave Motion* (to be published).

McWilliams, J., 1980: An application of equivalent modons to atmospheric blocking. *Dyn. Atmos. Oceans*, **5**, 219–238.

Miles, J. W., 1984: Parametrically excited solitary waves. *J. Fluid Mech.*, **148**, 451–460.

Pedlosky, J., 1987: *Geophysical Fluid Dynamics*, Springer–Verlag, 710pp.

Peixoto, J. P., B. Salztman, and S. Teweles, 1964: Harmonic analysis of the topography along parallels of the Earth. *J. Geophys. Res.*, **69**, 1501–1505.

Rex, D. F., 1950a: Blocking action in the middle troposphere and its effect upon regional climate, I: An aerological study of blocking action. *Tellus*, **2**, 196–301.

Rex, D. F., 1950b: Blocking action in the middle troposphere and its effect upon regional climate, II: The climatology of blocking action. *Tellus*, **2**, 275–301.

Shutts, G. J., 1983: The propagation of eddies in diffluent jetstreams: Eddy vorticity forcing of "blocking" flow fields. *Quart. J. Roy. Meteor. Soc.*, **109**, 737–761.

Swaters, G.E., 1986: Barotropic modon propagation over slowly varying topography. *Geophys. Astrophys. Fluid Dyn.*, **36**, 85–113.

Taba, T.R., and M.J. Ablowitz, 1984: Analytical and numerical aspects of certain nonlinear evolution equations. II: Numerical nonlinear Schrödinger equation. *J. Comput. Phys.*, **55**, 203–230.

Treidl, R.A., Birch, E.C., and P. Sajecki, 1981: Blocking action in the Northern Hemisphere: A climatological study. *Atmos. Ocean.*, **19**, 1–23.

Trevisan, A., and A. Buzzi, 1980: Stationary response of barotropic weakly nonlinear Rossby waves to quasi–resonant orographic forcing. *J. Atmos. Sci.*, **37**, 947–957.

Tung, K. K., and R. S. Lindzen, 1979: A theory of stationary long waves, Part I: A simple theory of blocking. *Mon. Wea. Rev.*, **107**, 714–734.

Warn, T., and Branset, B., 1983: The amplification and capture of atmosopheric solitons by topography: A theory of the onset of regional blocking. *J. Atmos. Sci.*, **40**, 28–38.

Yamagata, T., 1980: The stability, modulation and long wave resonance of a planetary wave in a rotating, two–layer fluid on a channel beta–plane. *J. Meteor. Soc. Japan.*, **58**, 160–171.

Appendix A

The coefficients of (13)–(15) are defined by

$$a_n = \frac{6}{m[(\frac{3}{2})^2 - n^2]L_y}, \quad b_n = \frac{2}{m[(\frac{1}{2})^2 - n^2]L_y}, \quad g_n = \frac{8}{m[4 - (n+\frac{1}{2})^2]L_y},$$

$$q_n = \frac{4k^2 m}{L_y}\{\beta + F\bar{u} - (\bar{u} - Cg)[F + (n+\frac{1}{2})^2 m^2]\},$$

$$p_1 = \frac{1}{2k(\beta + F\bar{u}) - [4k^2 + (\frac{3m}{2})^2 + F](2k\bar{u} - \omega)},$$

$$p_2 = \frac{3}{2k(\beta + F\bar{u}) - [4k^2 + (\frac{m}{2})^2 + F](2k\bar{u} - \omega)},$$

Appendix B

The coefficients of (17) are defined by

$$\lambda=\frac{[3(m^2+F)-k^2](\beta+F\bar{u})}{(k^2+m^2+F)^3},\quad \delta=\frac{km\sum_{n=1}^{\infty}[k^2+m^2-m^2(n+\frac{1}{2})^2]q_n g_n^2}{k^2+m^2+F},$$

$$R=\frac{k^2m(\frac{3}{4}m^2h_A+1)}{L_y\omega(k^2+m^2+F)}\sum_{n=1}^{\infty}\frac{(3a_n-b_n)n^2\{[(nm)^2-(k^2+\frac{m^2}{4})]h_A+1\}}{[(nm)^2+F](n^2-\frac{1}{4})(n^2-\frac{9}{4})},$$

$$S=-\frac{k^2m^2}{4(k^2+m^2+F)}(\frac{3}{4}m^2h_A+1)[(\frac{3k^2+2m^2}{4}p_1+\frac{9k^2}{4}p_2)h_A+\frac{p_1+3p_2}{4}],$$

$$R_1=\frac{\bar{u}-Cg-2k\lambda}{k^2+m^2+F},\quad R_2=\frac{\delta}{k}-\frac{2k\delta}{k^2+m^2+F}+q,\quad R_3=-q,$$

$$R_4=\delta_1-\frac{2kS}{k^2+m^2+F},$$

$$R_5=\delta_2-\frac{2kR}{k^2+m^2+F},\quad q=\frac{2k^2m}{k^2+m^2+F}\sum_{n=1}^{\infty}q_n g_n^2,$$

$$\delta_1=\frac{km^2(\frac{3}{4}m^2h_A+1)\{[(23k^2+2m^2)p_1-7k^2p_2]h_A+p_1-p_2\}}{16(k^2+m^2+F)},$$

$$\delta_2=\frac{km(\frac{3}{4}m^2h_A+1)}{8\omega L_y(k^2+m^2+F)}\sum_{n=1}^{\infty}\frac{(3a_n-b_n)(3-4n^2)\{[k^2+\frac{m^2}{4}-(nm)^2]h_A-1}{[(nm)^2+F](n^2-\frac{9}{4})(n^2-\frac{1}{4})}.$$

缓慢移动的行星尺度偶极子包络 Rossby 孤立子与双波地形相互作用

罗德海 李建平

摘 要

在 LG 型偶极子近共振条件下，获得了一个高阶非线性 Schrödinger 方程，并用此方程来描述缓慢移动的包络 Rossby 孤立子与双地形相互作用。数值结果表明，在 LG 型偶极子近共振条件下，在弱西风气流中，当一个弱包络孤立子位于地形槽区时，包络 Rossby 孤立子可以通过近共振强迫而放大，并产生振荡现象，然而长时间过后这个孤立子将破裂并激发一系列向西传播的小振幅波。在一定时间后，强迫孤立子除了东传外还存在一个缓慢的西传。同时，强迫包络 Rossby 孤立子的瞬时流场与观测到的 Ω 型阻高和偶极子的形成、维持和崩溃过程类似。除此之外，孤立子扰动理论被用来研究双波地形在 Ω 型阻高和偶极子中的作用。结果表明，在孤立子的强迫过程中，由于高阶项的存在，孤立子的群速度和相速趋于相等，以致于阻塞包络与载波在某个时刻锁相，在这种情况下，阻塞的产生是强迫包络孤立子从频散向非频散的转换过程，而在阻塞崩溃期间则相反。因此包络孤立子与地形相互作用可以认为是阻塞产生的可能机制。

关键词: 行星尺度包络 Rossby 孤立子，孤立子与地形相互作用，阻高